Proceedings of the 9th World Congress on Momentum, Heat and Mass Transfer (MHMT'24)
London, United kingdom – April 11 – 13, 2024
Paper No. ENFHT 200
DOI: 10.11159/enfht24.200

Ion Beam Induced Directional Flow of Ionic Liquid at Nanoscale

Haohao Gu[1], Kaixin Meng[1], Hao Wang[1]
[1]Laboratory of Heat and Mass Transport at Micro-Nano Scale, College of Engineering, Peking University,
Address, Beijing, 100871, P. R. China.
wanghpku@pku.edu.cn

Abstract
The branched flow pattern is ubiquitous in nature such as neuron structures, blood vessels and alluvial fans with the spatial scale ranges from micrometer to kilometer. Recently, we discover that such character still exists at nanometer scale and can be harnessed for the directional flow control of ionic liquids. At the proper irradiation of Helium Focused Ion Beam (HFIB), ionic liquid (IL) flows through local protrusions at contact line then branches off into secondary rivulets and forms hierarchical flow patterns. Such phenomenon is attributed to the field induced ion emission and nano meter scale precursor film. Molecular dynamics simulation results verify the important roles played by surface charges and precursor films in the directional propagation of ionic liquids. Moreover, the evolutions of the precursor films from MD simulations well reproduces the experimental results quantitatively. Such features endow programmable control of liquid flow and long endurance of fabricated liquid film patterns. We expect such mechanism can open a new avenue for microfluidic instruments and liquid nano circuit fabrications.

***Keywords*:** Branched flow, Ionic liquids, Focused ion beam, nanofluidics

1. Introduction

The dynamic behaviour of thin liquid films is important for many technological applications such as microfluidics, nano printing and energy generation. Branched flow patterns are ubiquitous in micro liquid systems, and is also known as fingering instability of flow which can jeopardize the spatial resolution of microfluidics instruments. The viscous fingering was first reported in a radial Hele-Shaw cell when a liquid with lower viscosity penetrates porous media filled with more viscous liquid[1], [2]. Such phenomenon is also called Saffman-Taylor problem, and arises because the less viscous fluid is more mobile than the more viscous fluid[3]. The similar fingering flow pattern was later reported in the thin film wetting experiments with surfactant concentration differences[4], [5]. The surfactant concentration leads to Marongoni stress which drive the directional propagation of thin liquid film and is responsible for an adverse mobility gradient which lead to the fingering instability of advancing liquid film. Apart from surfactant concentration gradients, the Marongoni effect can also be generated by temperature gradients, light beam irradiation and *etc*, with fingering instability also inevitable under such situations. Both the viscous induced fingering instability and the Marongoni induced fingering have the characteristic length scale at several micro meters[6], [7]. When Marongoni stress is harnessed for the directional transport of liquid and film pattern printing[7]–[9], the menisci of the liquid film fabricated would be restricted by the fingering instability effect and the spatial resolution of liquid film pattern is limited at micro meter scale.

Unlike the thermal and optical induced temperature gradients, the electron and ion beams can be readily focused to sub nano meter scale, and has been reported to be capable of triggering the movement of liquid at nano meter scale[10], [11]. Utkur M.M. *et al* reported that nano water droplet exhibit stick-slip motion at the irradiation of 120 keV electron beam generated by a Transmission Electron Microscope (TEM), although the direction and length of the movement were unpredictable. Such results revealed that the interaction between electron/ion beam and liquid material can also induce the directional movement of liquid while bypass the fingering instability effect.

In current work, we report that when ionic liquid (IL) is irradiated by the Helium Focused Ion Beam (HFIB) [12] with carefully prepared beam configurations, the liquid can be induced to flow through local protrusions at the liquid droplet contact line then branches off into secondary rivulets and forms hierarchical flow patterns. The branched flow pattern is similar to the fingering instability flow pattern but with totally different characteristic length scales. Such phenomenon is attributed to the field induced ion emission and nano meter scale precursor film. The surface charging injected by HFIB leads to the ion emission of IL and form ultrathin precursor film at desired region. We carefully characterize the branched flow process and Molecular Dynamics (MD) simulation is conducted. We prove that only well localized surface charges can

create stable precursor film at the irradiated surface region, while the constant electric field which has been widely adopted for ion emission and Taylor cone investigations[13], [14] cannot achieve the same results. The MD simulation results agree with the experimental observation and reveal that the characteristic length scale of the branched flow pattern is determined by the surface roughness elements of the solid substrates. The directional flow behaviour and nano meter scale flow character revealed in current work can be harnessed for the liquid film printing and nanofluidic instruments with little demands for surface fabrication procedures, which would largely reduce the flow control cost at nano meter scale.

2. Materials and Methods

2.1. Experimental materials and methods

The experimental system consists of a solid substrate, liquid reservoir and the Helium Ion Microscope (HIM, ORION NanoFab). The solid substrate is prepared as follow. An amorphous SiO_2 layer (3 μm) is deposited by plasma-enhanced chemical vapor deposition on a 500 μm quartz wafer. Before experiments, the solid substrate is cleaned with acetone, ethanol and ultrapure water with ultrasonication. A small droplet of 1-Ethyl-3-methylimidazolium Dicyanamide ([EMIM][DCA]) IL deposited on the substrate forms the liquid reservoir. The ionic liquid is dried in vacuum chamber at 80 ℃ for 24 h. After preparation, the samples are transferred into the vacuum chamber of HIM. The HIM provides the non-contact external stimulus, HFIB. With the imaging mode of HIM, the contact line (CTL) of IL droplet is identified as shown in Fig. 1a, b. Part of the CTL is chosen as the start position of HFIB scan as indicated by the yellow square in Fig. 1b, then the scan pattern is designed employing the Nano Patterning and Visualization Engine (NPVE) software which rasterize fills and scan the film pattern point-by-point (Fig 2a). After the irradiation of HFIB, the IL flows into the irradiated area and forms branched pattern as shown in Fig. 1c.

Table 1: HFIB parameters to induce liquid flow.

Beam parameters	Value
Accelerating voltage	30 kV
Beam current	0.1 ~ 1 pA
Dwell time	0.5 ~ 2 μs
Flood gun	On
Pixel size	1024×1024
Scan direction	Left-to-right in row, row by row outwards from contact line
Scan mode	Point by point

2.2. Molecular Dynamics simulation methods

The LAMMPS software is employed in current work as has been widely used in the investigation of liquid film wetting. As shown in Fig. 1d, two different force fields and molecular structures are employed to simulate the dynamic behaviour of ionic liquid droplet and film system. One is the all-atoms force fields developed by Padua and Lopes *et al* [15], and the other is the coarse-grained force field to reduce the computational cost[16]. The all-atoms system consists of 1500 ion pairs of [$EMIM^+$] [DCA^-] settled on a fused silica substrate and serve as the liquid reservoir to investigate the role played by surface charging effect in the formation of IL precursor film at the scanned area. Both surface charging at desired region and constant electric field are employed to drive the ion emission. The different results with similar electric field strength at the IL-vacuum interface help verify the roles played by localized surface charges injected by HFIB. The surface charging effect of HFIB is simulated by randomly created atoms with designated charge values to reproduce the Monte-Carlot simulation results from Ref. [17]. The surface charges are injected into the solid substrate right beneath the droplet CTL and relax for 1 ns, then the charges are removed and the

system relaxes for another 2 ns. After relaxation, new charges are injected and move outwards from the CTL. The injection-removing process is repeated for three times over the entire simulation.

The coarse-grained model is adopted to investigate the evolution process of the precursor film. A droplet consists of consists of 50000 pairs of coarse-grained ion pairs is settled and relaxed on top of a silica wafer with periodic roughness elements as shown in Fig. 1d. The height of the solid surface roughness element is 1.5 nm, and the periods in x and y directions are both 5 nm. To simulate the precursor film induced by the ion emission process, part of the ion pairs would be would be randomly created at the designed film area with same density as the surface charge density created by HFIB which is typically 5~8 pairs/nm^2. Then the droplet and film system relaxes for 5000 ns, with the film profiles analysed and compared with the experimental results. The size effect of solid roughness elements is investigated under the same simulation procedures with the lateral period and roughness height are adjusted. Figure 1e presents an example of the precursor film in front of the CTL of reservoir after relaxation.

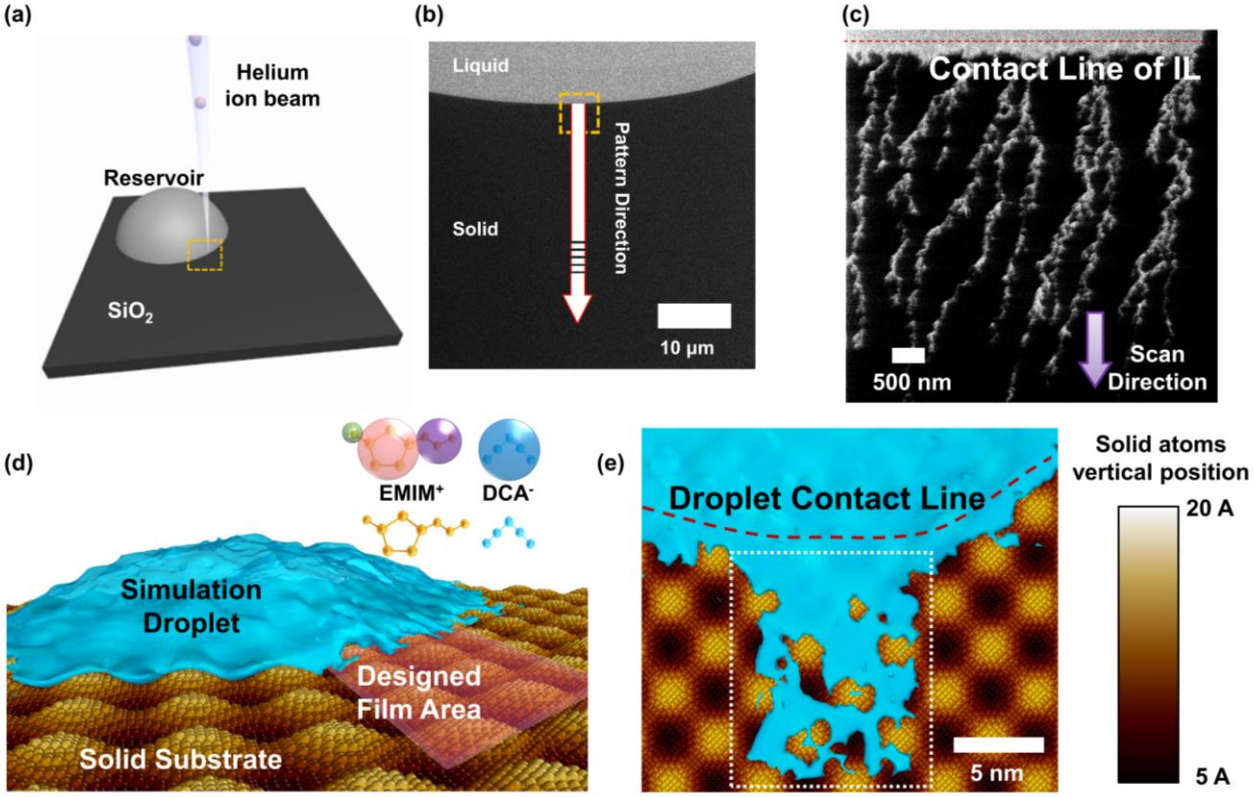

Fig. 1: The experiment and simulation schematics of ion beam induced directional flow. (a) the schematic of experimental system which consists of SiO_2 substrate, ionic liquid droplet reservoir and Helium focused ion beam as external stimulus. (b) the HIM image of the contact line region of a IL reservoir and the designed patterning area in NPVE. (c) the branched flow pattern of IL as a result of the scan of HFIB, the initial contact line of IL reservoir is marked by the red dashed line and the scan direction of HFIB is shown by the purple arrow. (d) the schematic of coarse-grained IL droplet settled on solid substrate with periodic roughness elements. The red rectangle represents the area designed to generate a precursor film of IL, the inset shows the structures of two different models adopted in current work. (e) the top view of the droplet contact line region and the precursor film after relaxation. The colour-bar represents the solid atoms vertical position ranging from 5 Å to 20 Å.

3. Results and Discussion

3.1. Experimental observation of branched flow at nanoscale

As described in section 2, the HFIB scans the designed area point by point in sequence as shown in Fig. 2a. After the patterning scan is over, the imaging mode of HIM is adopted to capture the real time image of the scanned area (Fig. 2b-h). The ionic liquid does not flow through the CTL line uniformly, but flow through some local protrusions at the CTL into the irradiated area instead. The positions of the protrusions are consistent with the convex region of CTL as shown by the yellow dashed circles in Fig. 2b-e. We speculate that the convex IL-vacuum interface reduces the free energy barrier for ions to overcome, and the significant ion emission at such region is more easily to take place at the same surface charge density. Consequently, the primary branches of IL flow form at the convex corrugations of CTL as seen in Fig. 2c-e. In Fig. 2c, the protrusions then branch off into secondary ones and form a hierarchical flow pattern in the HFIB scanned area. The propagation of branched flow pattern (Fig. 2c) takes place much faster than the widen of the flow branches that finally fills the entire scanned area (Fig. 2d-h). Eventually, the IL fill the entire region scanned by HFIB and well reproduces the straight line and sharp conner of the designed scan pattern (Fig. 2h). The Atomic Force Microscope results show that the fabricated liquid films are stable for days with the film thickness and film pattern barely changed (Fig. 4a).

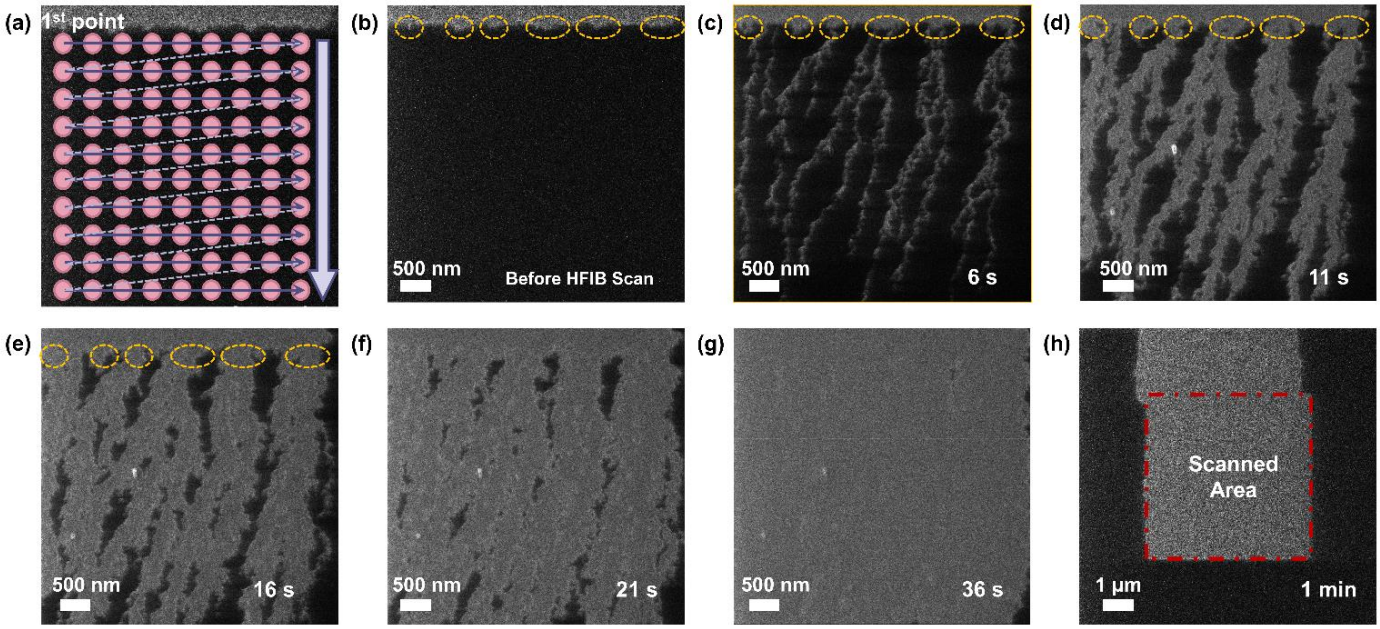

Fig. 2: Time series HIM images of the branched flow process of ionic liquid triggered by HFIB. IL flows over the contact line through several protrusions that located at the CTL and propagates separately as a series of long parallel 'rivulets' along the pattern direction (top-to-bottom). The rivulets branch off into secondary ones then multistage branching forms along the propagating direction. The exhibiting free-surface dendritic structures are completely distinct from commonly reported meniscus film fronts.

3.2. MD simulation of electric field and surface charges effects on IL

We speculate that ion emission process accounts for the directional flow of IL induced by HFIB irradiation. According to [13], the characteristic electric field strength for significant ion emission from IL-vacuum interface is $E^{*}{\sim}10^{9\sim10}\ V/m$. As shown in Fig. 3a, a constant electric field ($E^{*} = 10^{10}\ V/m$) is exerted at the contact line region of the IL reservoir, and ion emission can be observed within $10^{0\sim1} ps$ with both ions, clusters and even tiny droplets fast emitted from the droplet reservoir. But the emitted ions and liquid drops widely distribute over a wide spatial range and cannot be stabilized at desired region. However, by employing surface charges injection-removing process as discussed previously the ion emission can be controlled by the localized surface charging area and move simultaneously with the surface charges (Fig. 2b,c). Compared

with the constant electric field, the surface charges provide a well localized external field stimulus for ion emission and stabilize the precursor film with sub-nano meter thickness at desired region. Besides, the minimal liquid film pattern that can be induced by the HFIB irradiation is approximately 100 nm which is consistent with the surface charging distribution of HFIB scanned silica wafer. Both experimental and simulation results indicate that surface charge induced ion emission is important in the directional flow of IL induced by HFIB.

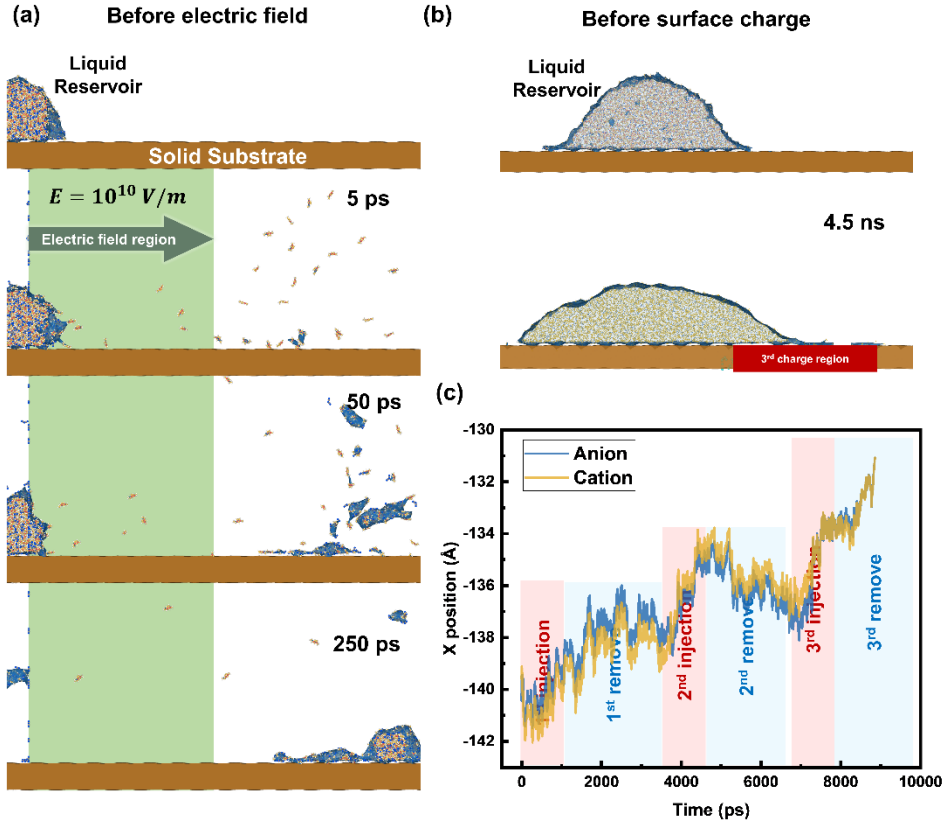

Fig. 3: Ionic liquid reservoir interacts with constant electric field and surface charging injection-removing process. (a) the constant electric field induce significant ion emission of IL reservoir, but fails to stabilize liquid film at desired region. (b) the localized surface charges induce controllable ion emission and stabilize precursor film in front of the CTL. (c) The x position of cations and anions mass-centre as a function of time. With the surface charges move to the positive direction, the IL move synchronically with a stepwise pattern.

3.3. Fractal dimension of IL films from experiment and MD simulation

We further characterize the shape complexity of liquid film propagation using fractal analysis, as shown in Fig. 4. The profiles of propagating liquid films are obtained and processed from three independent experiments. Fig. 4b is an example of the film profile extraction. The coarse-grained model is employed to investigate the film propagation process, and OVITO software is employed to process the simulation film profiles evolving with time (Fig. 2c). The fractal dimensions are calculated employing the box counting method with the results shown in Fig. 2a.

Experimental fractal dimension is depicted by the scatter plots in Fig. 3a. The shape complexity reaches maximum once the hierarchical flow pattern is formed (Fig. 2c), then gradually decays (Fig. 2d-f) and finally returns to the initial value when IL fills the entire scanned region (Fig. 2 g, h). The shape complexity first increases rapidly and reaches maximum when the liquid film first wetting the more hydrophilic surface and the fractal dimension is closely related to the solid surface characters. As the liquid flow into the scanned area and the branches widen, the secondary branches gradually emerge and

vanish. Consequently, the shape complexity of liquid film quickly decreases as the details of film patterns disappear and the fractal feature of the liquid film profile vanished.

The evolution of liquid film from coarse-grained simulation provides more details about the formation of the flow pattern (Fig. 4c). Since the solid surface have periodic roughness elements, the droplet has corrugations along the contact line (white dashed line in Fig. 4c). The pre-existed CTL protrusions extends into the designed scan region and the precursor film with the reservoir. Since the surface material is hydrophobic, the concave solid surface provides more interaction area for liquid molecules and consequently more hydrophilic compared with the convex region. Therefore, the liquid film preferentially propagates into the concave region of solid surface and forms a branched flow patterns as shown in Fig. 4c. The solid surface in experiments exhibit complex fractal roughness elements as shown in the inset of Fig. 4a. Therefore, the preferential flow pattern for IL film should exhibit more shape complexity, and can explain the differences between experiments and simulation in current work.

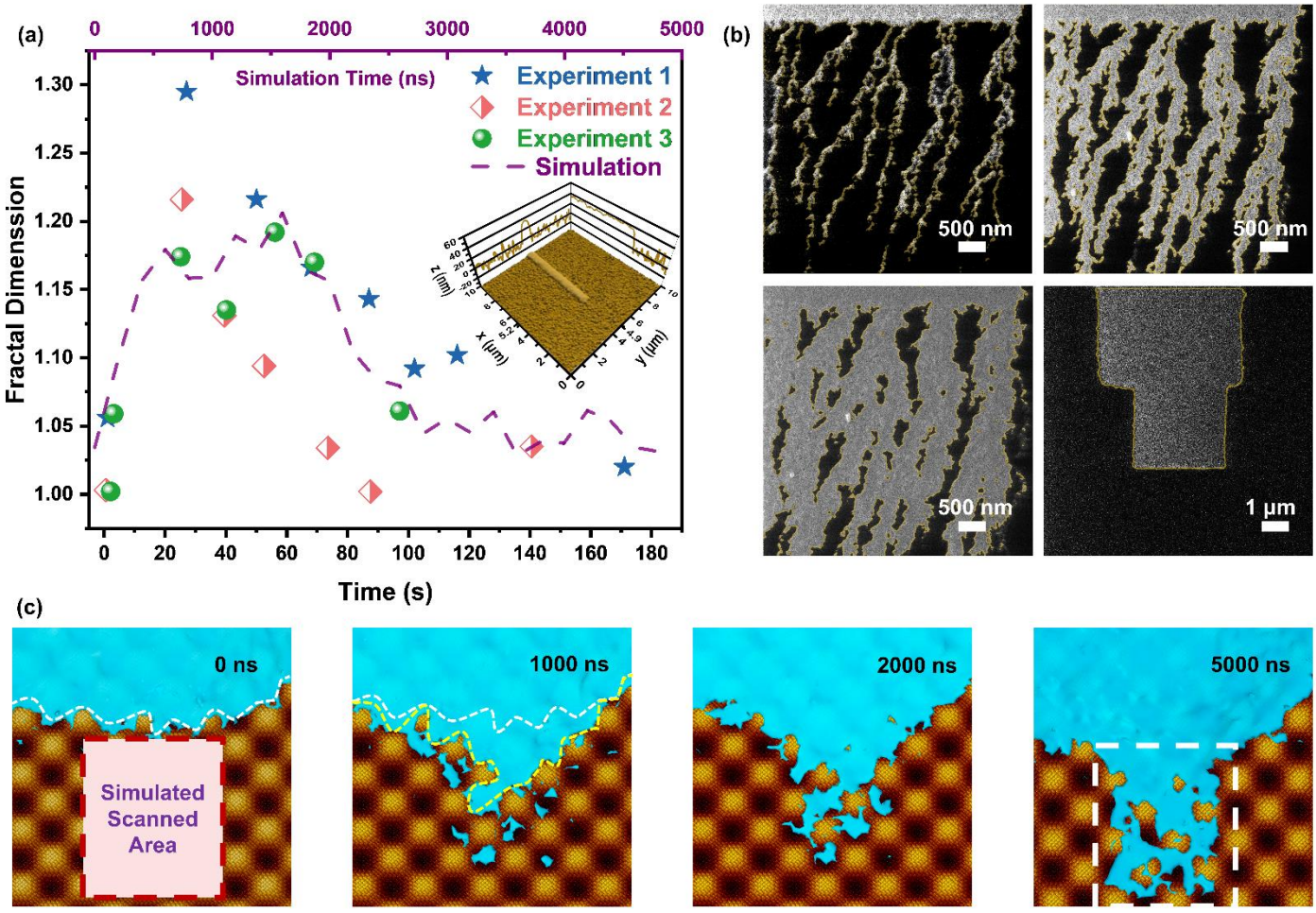

Fig. 4: Fractal dimension of branched liquid film in experiments and MD simulation. (a) The scatter plots represent the experimental results as shown in time series images in Fig. 4b. The purple dash line represents the simulation results. The inset is an AFM image of the HFIB induced liquid film, with 30 nm thickness and 1 μm width. (c) The evolution of liquid film in MD simulation. The liquid preferentially flows into the region that can interact with more solid atoms which explains the formation of the branched flow pattern at the beginning stage observed in experiments.

4. Conclusion

In current work, we reported that ionic liquids settled on a solid surface can flow into desired region at the proper irradiation of Helium focused ion beam without the aid of flow channels or physical masks. The branched flow pattern at at nano meter scale is discovered after the ionic liquid contact line is scanned by HFIB, which is distinguished from the viscous and Marangoni fingering instability reported previously. MD simulation results indicate that the surface charges injected by the HFIB induce localized ion emission of IL, then the preferential flow give rise to the branched flow pattern observed. The stabilized liquid films have 20 to 30 nm thickness, 100 nm spatial resolution and lifetime more than a week. Such features are important for the development of open surface nanofluidic instrument and nano printing technology.

Acknowledgements

This work was supported by National Natural Science Foundation of China (No. 51976001).

References

[1] G. Daccord, J. Nittmann, and H. E. Stanley, "Radial viscous fingers and diffusion-limited aggregation: Fractal dimension and growth sites," *Phys. Rev. Lett.*, vol. 56, no. 4, pp. 336–339, Jan. 1986, doi: 10.1103/PhysRevLett.56.336.

[2] P. G. Saffman and F. R. S. Sir geoffrey taylor, "The penetration of a fluid into a porous medium or Hele-Shaw cell containing a more viscous liquid," in *Dynamics of Curved Fronts*, P. Pelcé, Ed., San Diego: Academic Press, 1988, pp. 155–174. doi: 10.1016/B978-0-08-092523-3.50017-4.

[3] E. Álvarez-Lacalle, J. Ortín, and J. Casademunt, "Relevance of dynamic wetting in viscous fingering patterns," *Phys. Rev. E*, vol. 74, no. 2, p. 025302, Aug. 2006, doi: 10.1103/PhysRevE.74.025302.

[4] S. M. Troian, X. L. Wu, and S. A. Safran, "Fingering instability in thin wetting films," *Phys. Rev. Lett.*, vol. 62, no. 13, pp. 1496–1499, Mar. 1989, doi: 10.1103/PhysRevLett.62.1496.

[5] A. B. Afsar-Siddiqui, P. F. Luckham, and O. K. Matar, "The spreading of surfactant solutions on thin liquid films," *Advances in Colloid and Interface Science*, vol. 106, no. 1, pp. 183–236, Dec. 2003, doi: 10.1016/S0001-8686(03)00111-8.

[6] A. M. Cazabat, F. Heslot, S. M. Troian, and P. Carles, "Fingering instability of thin spreading films driven by temperature gradients," *Nature*, vol. 346, no. 6287, Art. no. 6287, Aug. 1990, doi: 10.1038/346824a0.

[7] G. L. Liu, J. Kim, Y. Lu, and L. P. Lee, "Optofluidic control using photothermal nanoparticles," *Nat Mater*, vol. 5, no. 1, Art. no. 1, Jan. 2006, doi: 10.1038/nmat1528.

[8] N. Garnier, R. O. Grigoriev, and M. F. Schatz, "Optical Manipulation of Microscale Fluid Flow," *Phys. Rev. Lett.*, vol. 91, no. 5, p. 054501, Jul. 2003, doi: 10.1103/PhysRevLett.91.054501.

[9] A. Casner and J.-P. Delville, "Laser-Induced Hydrodynamic Instability of Fluid Interfaces," *Phys. Rev. Lett.*, vol. 90, no. 14, p. 144503, Apr. 2003, doi: 10.1103/PhysRevLett.90.144503.

[10] U. M. Mirsaidov, H. Zheng, D. Bhattacharya, Y. Casana, and P. Matsudaira, "Direct observation of stick-slip movements of water nanodroplets induced by an electron beam," *Proceedings of the National Academy of Sciences*, vol. 109, no. 19, pp. 7187–7190, May 2012, doi: 10.1073/pnas.1200457109.

[11] P. Ferraro, S. Coppola, S. Grilli, M. Paturzo, and V. Vespini, "Dispensing nano–pico droplets and liquid patterning by pyroelectrodynamic shooting," *Nat Nanotechnol*, vol. 5, no. 6, Art. no. 6, Jun. 2010, doi: 10.1038/nnano.2010.82.

[12] P.-C. Shen, C. Su, Y. Lin, A.-S. Chou, C.-C. Cheng, J.-H. Park, M.-H. Chlu, A.-Y. Lu, H.-L. Tang, M. M. Tavakoli, G. Pitner, X. Ji, Z. Cai, N. Mao, J. Wang, V. Tung, J. Li, J. Bokor, A. Zettl, C. Wu, T. Palacios, L.-J. Li, and J. Kong "Ultralow contact resistance between semimetal and monolayer semiconductors," *Nature*, vol. 593, no. 7858, Art. no. 7858, May 2021, doi: 10.1038/s41586-021-03472-9.

[13] C. S. Coffman, M. Martínez-Sánchez, and P. C. Lozano, "Electrohydrodynamics of an ionic liquid meniscus during evaporation of ions in a regime of high electric field," *Phys Rev E*, vol. 99, no. 6, p. 063108, Jun. 2019, doi: 10.1103/PhysRevE.99.063108.

[14] F. Zhang, X. Jiang, G. Chen, Y. He, G. Hu, and R. Qiao, "Electric-Field-Driven Ion Emission from the Free Surface of Room Temperature Ionic Liquids," *J. Phys. Chem. Lett.*, vol. 12, no. 1, pp. 711–716, Jan. 2021, doi: 10.1021/acs.jpclett.0c03335.
[15] J. N. Canongia Lopes, J. Deschamps, and A. A. H. Pádua, "Modeling Ionic Liquids Using a Systematic All-Atom Force Field," *J. Phys. Chem. B*, vol. 108, no. 6, pp. 2038–2047, Feb. 2004, doi: 10.1021/jp0362133.
[16] D. Roy and M. Maroncelli, "An Improved Four-Site Ionic Liquid Model," *J. Phys. Chem. B*, vol. 114, no. 39, pp. 12629–12631, Oct. 2010, doi: 10.1021/jp108179n.
[17] T. Ishitani, T. Yamanaka, K. Inai, and K. Ohya, "Secondary electron emission in scanning Ga ion, He ion and electron microscopes," *Vacuum*, vol. 84, no. 8, pp. 1018–1024, Mar. 2010, doi: 10.1016/j.vacuum.2009.12.010.